Substrate dependence of graphene reactivity towards hydrogenation

Cite as: Appl. Phys. Lett. **109**, 243103 (2016); https://doi.org/10.1063/1.4971385
Submitted: 23 August 2016 • Accepted: 24 October 2016 • Published Online: 15 December 2016

S. Son, C. Holroyd, J. Clough, et al.

Substrate dependence of graphene reactivity towards hydrogenation

S. Son,[1,2] C. Holroyd,[2] J. Clough,[2] A. Horn,[2] S. P. K. Koehler,[2,3] and C. Casiraghi[2]
[1]*School of Physics and Astronomy, The University of Manchester, Manchester M13 9PL, United Kingdom*
[2]*School of Chemistry, The University of Manchester, Manchester M13 9PL, United Kingdom*
[3]*Photon Science Institute, The University of Manchester, Manchester M13 9PL, United Kingdom*

(Received 23 August 2016; accepted 24 October 2016; published online 15 December 2016)

The ability to functionalize graphene with several methods, such as radical reactions, cycloadditions, hydrogenation, and oxidations, allows this material to be used in a large range of applications. In this framework, it is essential to be able to control the efficiency and stability of the functionalization process—this requires understanding how the graphene reactivity is affected by the environment, including the substrate. In this work we provide an insight on the substrate dependence of graphene reactivity towards hydrogenation by comparing three different substrates: silicon, hexagonal boron nitride (h-BN), and molybdenum disulfide (MoS_2). Although MoS_2 and h-BN have flatter surfaces than silicon, we found that the H coverage of graphene on h-BN is about half of the H coverage on graphene on both silicon and MoS_2. Therefore, graphene shows strongly reduced reactivity towards hydrogenation when placed on h-BN. The difference in hydrogenation reactivity between h-BN and MoS_2 may indicate a stronger van der Waals force between graphene and h-BN, compared to MoS_2, or may be related to the chemical properties of MoS_2, which is a well-known catalyst for hydrogen evolution reactions.
[http://dx.doi.org/10.1063/1.4971385]

Graphene is a 2-Dimensional (2-D) hexagonal lattice of carbon atoms that is attracting great attention because of its unique properties and potential applications.[1–3] Graphene, being a surface, is strongly sensitive to the environment: this allows fine tuning the properties of graphene by covalent methods.[4,5] Those include chemical reactions, such as diazo-coupling, polymerization, cyclo-addition, and plasma treatment, which allows the attachment of atoms such as hydrogen[6,7] to the graphene scaffold.

Functionalisation processes based on plasma are simple and attractive methods for the modification of graphene surface with various atoms.[8,9] However, the functionalization mechanism via plasma treatment is not completely understood. It is believed that carbon atoms at corrugated parts, edges, defects, etc., are more reactive than carbon atoms in the basal plane.[10] In the case of hydrogenation, the C–H bond formation leads to a change in the local atomic structure, producing a strained and buckled surface around the C–H bond. This local area is considered the "nucleation point" for the hydrogenation to start. However, several experiments have indicated that this simple theory may not be able to fully explain the reactivity of graphene towards hydrogenation. Diankov *et al.*[11] have compared graphene subjected to H plasmas onto two different substrates: silicon and mica. Although mica is smoother than silicon, no differences were observed between the two substrates. Charge puddles in the silicon substrate have been considered responsible for the enhanced chemical reactivity of graphene, compared to graphene multi-layers.[11,12] We remark however that in those studies, the plasma treatment was used to etch graphene, while covalent functionalization requires different ion energy distributions. In any case, these initial works indicate that the substrate has a crucial importance in determining the reactivity of graphene.

One of the most used substrates is hexagonal boron nitride (h-BN) as it allows achieving the highest charge mobility for supported graphene.[13] However, with the isolation of 2-D materials beyond graphene and the introduction of "2-D-crystal based heterostructures",[14] graphene is now placed also on other substrates; some of them have been shown to be detrimental to the electronic properties of graphene due to contamination and bad quality of the interfaces.[15,16] In this framework, it is therefore important to further investigate how the surface properties and chemistry of the substrate affect graphene reactivity. A recent work[17] reports a study on the chemical reactivity of single and bilayer graphene (SLG and BLG, respectively) deposited on silicon (SiO_2), dichalcogenides (MoS_2 and WS_2) and h-BN. Hydrogenation was performed by using a chemical method based on hydrogen silsesquioxane. The authors attribute the higher chemical stability of SLG, when deposited to another 2-D crystal, compared to silicon, to the stronger van der Waals interaction between graphene and the 2-D substrate by providing a higher resistive force towards geometric lattice deformation.[17] This effect is believed to be more dominant than both local curvature and charged puddle effects.[17]

In this letter we show a direct comparison of hydrogenated graphene on the following substrates: silicon (Si) with 290 nm thick silicon dioxide (Gr/SiO_2), molybdenum disulfide (Gr/MoS_2), and hexagonal boron nitride (Gr/h-BN). We show that h-BN minimises the reactivity of graphene to hydrogenation, while graphene on MoS_2 shows hydrogenation reactivity

comparable to that observed for silicon. The H coverage of graphene on h-BN is found to be about half of the H coverage on silicon and MoS_2.

The graphene crystals (a few hundreds of microns in size) and thin flakes of MoS_2 and h-BN were produced by micro-mechanical exfoliation on a standard silicon substrate with 290 nm SiO_2.[18] The pristine graphene samples obtained have been characterized by Raman spectroscopy in order to make sure that they all have comparable quality. In particular, the intensity ratio between the 2D and G peak was used as a benchmark to assess the quality (in our case, values around 1.8 have been found for all graphene flakes transferred onto silicon). Those graphene flakes were transferred from silicon by using a dry-peel transfer.[15] Figures 1(a) and 1(b) shows the optical pictures of Gr/MoS_2 and Gr/h-BN samples. Note that the graphene crystal was partially transferred on MoS_2 and h-BN in order to allow direct comparison between silicon and MoS_2 or h-BN. The samples were exposed to hydrogen plasma made by using a modified Edwars E306A coating system chamber. A hydrogen-argon mixture (10% H_2) at a pressure of ~0.1 mbar was employed and a dc plasma ignited between two aluminium electrodes. The samples were placed about 30 cm away from the discharge zone in order to minimize any possible damage due to energetic ions. Both samples were placed in the chamber at the same time and next to each other, so they were exposed exactly to the same plasma conditions. Graphene was hydrogenated for 60 min.

Atomic Force Microscopy (AFM) was performed on a $5 \times 5\ \mu m^2$ area in order to investigate the surface properties of the samples before and after hydrogenation. Figures 1(c) and 1(d) show the AFM pictures of the samples Gr/MoS_2 and Gr/h-BN, respectively. The root mean square (RMS) roughness of graphene on MoS_2, h-BN, and on silicon is 0.46 nm, 0.34 nm, and 0.71 nm, respectively. The thickness of the MoS_2 and h-BN flakes is 24 nm and 21 nm, respectively. A few bubbles are visible, as often observed for transferred graphene,[15] but the area is largely clean, and no damage or other surface deformations are visible under the optical microscope.

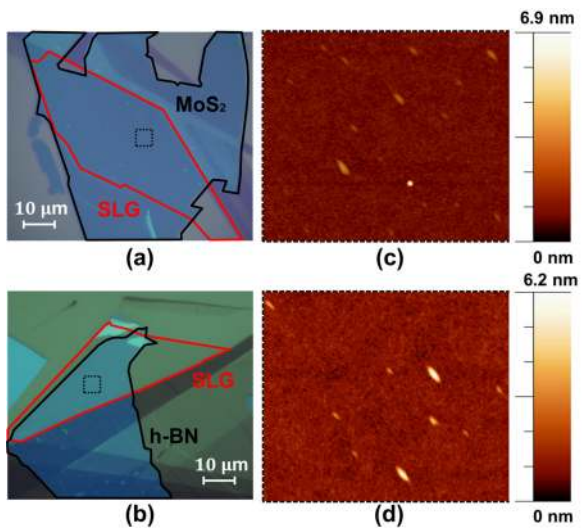

FIG. 1. Optical micrograph and AFM images of the samples. Graphene transferred on MoS_2 flake (a) and on h-BN flake (b). In both cases, the crystal partially overlaps with the Si substrate. The closed-red-line indicates the graphene flake and the closed-black-line is the MoS_2 and h-BN flake in (a) and (b), respectively. AFM images of Gr/MoS_2 (c) and Gr/ h-BN (d), measured in the dotted square in (a) and (b), respectively. The AFM scanned area is $5 \times 5\ \mu m^2$.

A Renishaw Raman spectrometer, equipped with excitation lines of 514 nm and 633 nm, was used to identify graphene[19] and to determine hydrogenation conditions.[7] The incident power was maintained below 2 mW during the measurement to avoid any possible damage and heating of samples, which may lead to hydrogen removal. In contrast to other types of functionalization methods, the formation of C−H bonds is a reversible process: the hydrogen can be desorbed from the graphene scaffold through the application of thermal energy.[7] Therefore, hydrogenation can be easily verified by annealing the samples (we used a 300 °C in the mixed argon and hydrogen gas flow for 5 h) and by performing Raman spectroscopy. There are two prominent peaks in the Raman spectrum of graphene, known as the G peak and the 2D peak, at ~1580 cm^{-1} and ~2700 cm^{-1}, respectively.[19] Raman spectroscopy is strongly sensitive to defects in graphene, as they activate characteristic modes, called D and D′ peaks, at ~1340 cm^{-1} and ~1620 cm^{-1}, respectively.[20,21] After annealing of the samples, the Raman spectrum recovered its original shape, Figure 2 (blue and black spectra), confirming hydrogenation under the conditions used in this work.

Note that Gr/MoS_2 and Gr/h-BN samples have been measured at 514 nm and 633 nm wavelength, respectively, see Figure 2. Raman spectroscopy cannot be performed under the same experimental conditions for the two samples: when graphene is placed on h-BN it is necessary to use 633 nm excitation wavelength in order to clearly distinguish the D peak from the h-BN peak, at ~1350 cm^{-1}. On the other hand, when graphene is placed on MoS_2, 514 nm excitation wavelength has to be used to avoid the photoluminescence background coming from the MoS_2. However, the Raman spectrum of graphene is strongly dependent on the excitation wavelength[20,21] so it is not possible to directly compare the Raman spectra of Gr/MoS_2 and Gr/h-BN. As both samples partially overlap on the Si substrate, this can be used as a reference to indirectly

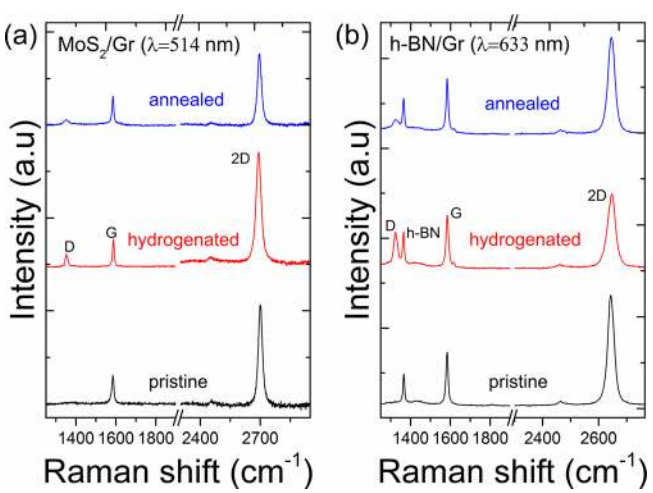

FIG. 2. Raman spectra of graphene, hydrogenated graphene, and annealed graphene on MoS_2 and h-BN. Raman spectra of Gr/MoS_2 (a) and Gr/h-BN (b). The spectra are normalised to the G peak intensity. Black, red, and blue spectra indicate pristine, hydrogenated, and annealed samples, respectively.

compare the reactivity of graphene on MoS_2 and h-BN. The comparison between samples can be made by taking into account that an increasing amount of defects on the Raman spectrum of graphene can be described with a phenomenological three-stage amorphization trajectory.[20–23] In stage 1, starting from pristine graphene, the Raman spectrum evolves as follows: the D peak appears and the intensity ratio between the D and G peaks [I(D)/I(G)] increases; the D′ appears; all the peaks broaden and G and D′ begin to overlap. In this stage, I(D)/I(G) can be used to estimate the amount of defects,[20,24] while I(D)/I(D′) can be used to distinguish between the different types of defects.[25] At the end of Stage 1, the G and D′ peaks are no more distinguishable, I(D)/I(G) starts decreasing. As the number of defects keep increasing, the Raman spectrum enters Stage 2, showing a marked decrease in the G peak position and increase broadening of the peaks; I(D)/I(G) sharply decreases towards zero and second-order peaks are no longer well defined. Stage 3 describes amorphous materials with increasing sp^3 content.[22,23] For supported graphene, where only one side of the crystal is available for functionalization, hydrogenation is obtained in stage 1, therefore I(D)/I(G) increases with an increasing amount of defects (i.e., H coverage); this allows us to use I(D)/I(G) to measure the graphene reactivity towards hydrogenation.

Because hydrogenation is not uniform over the graphene surface,[10] a single Raman spectrum may not be representative of the functionalization process. We used Raman mapping to get the I(D)/I(G) distribution over a clean area of $\sim 5\ \mu m \times 5\ \mu m$, without any bubble or visible deformation. Figures 3(a) and 3(b) show the I(D)/I(G) maps of hydrogenated graphene on MoS_2 and Si, measured on the Gr/MoS_2 sample in Figure 1(a). Figures 3(c) and 3(d) show the I(D)/I(G) maps of hydrogenated graphene on h-BN and Si, measured on the Gr/h-BN sample in Figure 1(b). Figures 3(e) and 3(f) show the histograms of I(D)/I(G) extracted from the maps in Figures 3(a)–3(d). This figure can be used to compare the three substrates: the average I(D)/I(G) of graphene on MoS_2 is 0.608, similar to the value obtained for the silicon substrate (0.614). This indicates that the reactivity to hydrogenation of graphene on MoS_2 is comparable with that of graphene on silicon. The average I(D)/I(G) of graphene on h-BN is 0.69, is almost half of I(D)/I(G) measured on the silicon substrate (1.23). As mentioned earlier, I(D)/I(G) of Gr/MoS_2 and Gr/h-BN samples cannot be compared because measured at different excitation wavelengths. However, I(D)/I(G) is known to increase with increasing laser wavelengths,[20,21] so a similar I(D)/I(G) between h-BN and MoS_2 measured at 633 and 514 nm, respectively, indicates that h-BN strongly minimises graphene reactivity towards hydrogenation.

In order to remove the dependence on the excitation wavelength, we convert I(D)/I(G) into H coverage. Ref. 20 proposed a relation between defect concentration (n) and I(D)/I(G) as: $L_D^2\ (nm^2) = (1.8 \pm 0.5) \times 10^{-9}\ \lambda_L^4 \times [I(D)/I(G)]^{-1}$ and $n_D\ (cm^{-2}) = 10^{14}/(\pi L_D^2)$ where L_D is separation between defects, λ_L is the laser wavelength, and n_D is the number of defects/cm^2. However, this relation was found for ion-bombarded graphene samples.[20] In the case of hydrogenation, upon chemisorption of the first H atom on the graphene lattice, the following H atoms will bond to cluster around the initial chemisorbed H atom, which acts as the nucleation point. Therefore, n_D found by using the relation proposed in Ref. 20 needs to be multiplied by a correction factor, which takes into account, the clusters formation. By calculating the total number of carbon sites available for hydrogenation as a function of the cluster size (assumed circular in shape and smaller than the defects distance of ~ 5 nm, which sets the crossing between Stage 1 and 2), we deduced a correction factor of ~ 175, in good agreement with previous works.[26,27] In this way, we found H coverage of $1.3 \pm 0.3\%$ for both

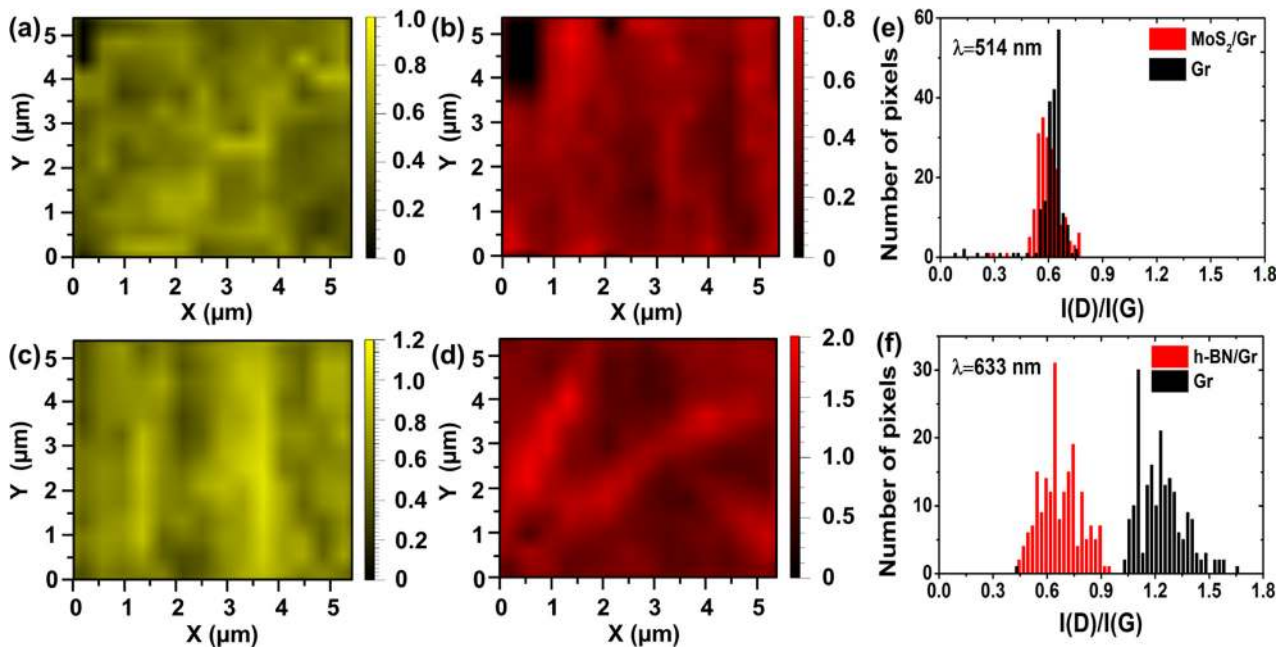

FIG. 3. Raman maps of I(D)/I(G) of hydrogenated graphene on different substrates. I(D)/I(G) maps of hydrogenated graphene on MoS_2 (a) and on silicon substrate for the Gr/MoS_2 sample (b). I(D)/I(G) maps of hydrogenated graphene on h-BN (c) and on silicon substrate for the Gr/h-BN sample (d). Note that different excitation wavelengths are used for the two samples, so the values are not directly comparable. (e) and (f) Histograms of I(D)/I(G) extracted from the maps in (a)–(d).

TABLE I. Summary of the H coverage obtained for graphene on silicon, MoS_2, and h-BN from the Raman spectra measured on the two samples investigated [Gr/Mos_2 and Gr/h-BN].

Sample	λ (nm)	I(D)/I(G)	Coverage (%)
Hydrogenated Gr on Si [Gr/MoS_2]	514.5	0.614	~1.3
Hydrogenated Gr on MoS_2 [Gr/MoS_2]	514.5	0.608	~1.3
Hydrogenated Gr on Si [Gr/h-BN]	633	1.23	~1.2
Hydrogenated Gr on h-BN [Gr/h-BN]	633	0.69	~0.7

graphene on MoS_2 and silicon, in contrast to graphene on h-BN, which shows H coverage of only $0.7 \pm 0.3\%$. Table I summarizes the results obtained. This result indicates that h-BN strongly minimizes the reactivity of graphene towards hydrogenation and further confirms h-BN as the most suitable substrate for fabrication of graphene-based devices.[13] This is also in agreement with the results in Ref. 28, where graphene devices on different substrates have been compared: the highest mobility at room temperature was observed when graphene is placed on h-BN ($\sim 38\,000\,cm^2\,V^{-1}\,s^{-1}$), followed by WS_2 and then MoS_2. The latter shows mobility comparable to that obtained when graphene is placed on the oxidized Si substrate.

In conclusion, our study provides further insights into the effect of the substrate on the hydrogenation reactivity of graphene. Our results indicate that graphene shows a strongly reduced reactivity towards hydrogenation when placed on h-BN, while MoS_2 gives rise to a similar reaction rate as compared to silicon. Although MoS_2 and h-BN have flatter surfaces than silicon, the H coverage of graphene on h-BN is found to be about half of the H coverage on both silicon and MoS_2, when exposed under the same experimental conditions. The difference in hydrogenation reactivity between h-BN and MoS_2 may indicate a stronger van der Waals force between graphene and h-BN,[17] compared to MoS_2, or may be related to the chemical properties of MoS_2, which is a well known catalyst for hydrogen evolution reactions.[29]

S.S. and C.C. acknowledge financial support by the Army Research Office. C.H., J.C., A.H., S.S., and C.C. acknowledge the EPSRC in the framework of the DTA scholarship. S.S. would like to thank Y. Shin for useful discussions and advice.

[1]A. K. Geim and K. S. Novoselov, Nat. Mater. **6**, 183–191 (2007).
[2]A. K. Geim, Science **324**, 1530–1534 (2009).
[3]K. S. Novoselov, V. I. Fal'ko, L. Colombo, P. R. Gellert, M. G. Schwab, and K. Kim, Nature **490**, 192–200 (2012).
[4]C. K. Chua and M. Pumera, Chem. Soc. Rev. **42**, 3222 (2013).
[5]A. Criado, M. Melchionna, S. Marchesan, and M. Prato, Angew. Chem., Int. Ed. **54**, 10734 (2015).
[6]K. S. Subrahmanyam, P. Kumar, U. Maitra, A. Govindaraj, K. P. S. S. Hembram, U. V. Waghmare, and C. N. R. Rao, Proc. Natl. Acad. Sci. U.S.A. **108**, 2674–2677 (2011).
[7]D. C. Elias, R. R. Nair, T. M. G. Mohiuddin, S. V. Morozov, P. Blake, M. P. Halsall, A. C. Ferrari, D. W. Boukhvalov, M. I. Katsnelson, A. K. Geim *et al.*, Science **323**, 610 (2009).
[8]A. Felten, A. Eckmann, J.-J. Pireaux, R. Krupke, and C. Casiraghi, Nanotechnology **24**, 355705 (2013).
[9]A. Felten, B. S. Flavel, L. Britnell, A. Eckmann, P. Louette, J.-J. Pireaux, M. Hirtz, R. Krupke, and C. Casiraghi, Small **9**, 631–639 (2013).
[10]D. Boukhvalov and M. Katsnelson, J. Phys. Chem. C **113**, 14176–14178 (2009).
[11]G. Diankov, M. Neumann, and D. Goldhaber-Gordon, ACS Nano **7**, 1324–1332 (2013).
[12]M. Yamamoto, T. Einstein, M. Fuhrer, and W. Cullen, ACS Nano **6**, 8335–8341 (2012).
[13]C. R. Dean, A. F. Young, I. Meric, C. Lee, L. Wang, S. Sorgenfrei, K. Watanabe, T. Taniguchi, P. Kim, K. L. Shepard *et al.*, Nat. Nanotechnol. **5**, 722–726 (2010).
[14]A. K. Geim and I. V. Grigorieva, Nature **499**, 419–425 (2013).
[15]A. V. Kretinin, Y. Cao, J. S. Tu, G. L. Yu, R. Jalil, K. S. Novoselov, S. J. Haigh, A. Gholinia, A. Mishchenko, M. Lozada *et al.*, Nano Lett. **14**, 3270–3276 (2014).
[16]K.-G. Zhou, F. Withers, Y. Cao, S. Hu, and C. Casiraghi, ACS Nano **8**, 9914–9924 (2014).
[17]J. H. Lee, A. Avsar, J. Jung, J. Y. Tan, K. Watanabe, T. Taniguchi, S. Natarajan, G. Eda, S. Adam, A. H. Castro Neto *et al.*, Nano Lett. **15**, 319–325 (2015).
[18]K. S. Novoselov, D. Jiang, F. Schedin, T. J. Booth, V. V. Khotkevich, S. V. Morozov, and A. K. Geim, Proc. Natl. Acad. Sci. U.S.A. **102**, 10451–10453 (2005).
[19]A. C. Ferrari, J. C. Meyer, V. Scardaci, C. Casiraghi, M. Lazzeri, F. Mauri, S. Piscanec, D. Jiang, K. S. Novoselov, S. Roth *et al.*, Phys. Rev. Lett. **97**, 187401 (2006).
[20]L. G. Cançado, A. Jorio, E. H. M. Ferreira, F. Stavale, C. A. Achete, R. B. Capaz, M. V. O. Moutinho, A. Lombardo, T. S. Kulmala, and A. C. Ferrari, Nano Lett. **11**, 3190–3196 (2011).
[21]A. Eckmann, A. Felten, I. Verzhbitskiy, R. Davey, and C. Casiraghi, Phys. Rev. B **88**, 035426 (2013).
[22]A. C. Ferrari and J. Robertson, Phys. Rev. B **64**, 075414 (2001).
[23]C. Casiraghi, A. C. Ferrari, and J. Robertson, Phys. Rev. B **72**, 085401 (2005).
[24]E. H. M. Ferreira, M. V. O. Moutinho, F. Stavale, M. M. Lucchese, R. B. Capaz, C. A. Achete, and A. Jorio, Phys. Rev. B **82**, 125429 (2010).
[25]A. Eckmann, A. Felten, A. Mishchenko, L. Britnell, R. Krupke, K. S. Novoselov, and C. Casiraghi, Nano Lett. **12**, 3925 (2012).
[26]V. G. Kravets, R. Jalil, Y.-J. Kim, D. Ansell, D. E. Aznakayeva, B. Thackray, L. Britnell, B. D. Belle, F. Withers, I. P. Radko *et al.*, Sci. Rep. **4**, 5517 (2014).
[27]V. G. Kravets, F. Schedin, R. Jalil, L. Britnell, R. V. Gorbachev, D. Ansell, B. Thackray, K. S. Novoselov, A. K. Geim, A. V. Kabashin *et al.*, Nat. Mater. **12**, 304–309 (2013).
[28]J. Y. Tan, A. Avsar, J. Balakrishnan, G. K. W. Koon, T. Taychatanapat, E. C. T. O'Farrell, K. Watanabe, T. Taniguchi, G. Eda, A. H. Castro Neto *et al.*, Appl. Phys. Lett. **104**, 183504 (2014).
[29]D. Voiry, M. Salehi, R. Silva, T. Fujita, M. Chen, T. Asefa, V. B. Shenoy, G. Eda, and M. Chhowalla, Nano Lett. **13**, 6222 (2013).